ELSEVIER

Materials Science and Engineering A209 (1996) 206–212

MATERIALS SCIENCE & ENGINEERING A

Oxidation behavior of WC–Co

S.N. Basu, V.K. Sarin

Manufacturing Engineering Department, Boston University, Boston, MA 02215, USA

Abstract

The high temperature oxidation behavior of WC–Co samples has been investigated. The oxidation rate of WC–Co was found to increase rapidly with temperature above 600 °C and with the oxygen content of the atmosphere. Increasing the Co content led to an improvement in the oxidation behavior. In all cases, only WO_3 and $CoWO_4$ phases were present in the oxide. Although the morphology of the two oxide phases depended on the oxidation conditions, their volume fractions were determined solely by the Co content of the sample. The WO_3 formed during the initial stages of oxidation, changed from a strong {001} texture at 600 °C to a weak {200} texture at 800 °C. As the flow rate of the oxidizing gas was increased, the oxidation rate of WC–Co increased at lower flow rates due to an increase in the oxygen supply to the oxide/sample interface. However, at higher flow rates, the oxidation rates decreased with increasing flow rate.

Keywords: Oxidation behaviour; Cobalt; Temperature; Cemented carbides; Microstructure

1. Introduction

With an increase in the cutting speed of cemented carbide cutting tools, temperatures at the tool/chip interface can become quite high, in some cases in excess of 1000 °C [1,2]. Thus, oxidation of cemented carbides can become a contributor to tool wear. Limited studies of the oxidation behavior of cemented carbides have been carried out to date. Padilla and co-workers [3] reported that oxidation and chemical attack is the major cause of tool wear during machining of medium density fiberboard [3]. They found the oxidation kinetics of WC–Co to be linear, with an exponential increase with temperature. The authors also reported that oxidation occurred at temperatures as low as 500 °C, and that there was a loss of WO_3 vapors at 1000 °C. Bhaumik et al. [4] studied the effect of TiC, TiN, Mo_2C and Ni additions on the isothermal oxidation of WC–Co samples at 800 °C in air. They reported that, based on weight gain data, adding TiN and TiC to WC–Co and substituting Ni for Co in the binder phase improved oxidation behavior.

This paper describes the results of a systematic study of the oxidation behavior of WC–Co. The parameters varied in this study include the binder phase concentration; oxygen content of the atmosphere; temperature; and flow rate of the oxidizing gas.

2. Experimental procedures

Coarse grained WC–Co (WC grain size of approximately 8 μm) samples were oxidized isothermally in flowing Ar–O_2 gas mixtures at temperatures of 600, 700 and 800 °C. To study the effect of the binder phase on oxidation, samples with 6 and 12 wt.% Co (all concentrations reported hereafter are in wt.%) were used. The oxygen content in the gas mixture was varied from 10% to 50% by volume, and the total flow rates ranged from 0.1 to 2 l min^{-1} under standard conditions of 278 K and 1 atmosphere pressure (all flow rates reported hereafter are under standard conditions).

The flow rates of Ar and O_2 were controlled by individual mass flow controllers. The gases were thoroughly premixed before being introduced through the bottom of a quartz reaction chamber, approximately 5 cm in diameter. The bottom of the reaction tube was packed with quartz chips to ensure uniform flow within the tube. Oxidation coupons, $10 \times 10 \times 3$ mm^3 in size, were suspended within the reaction tube by a Pt wire from a CAHN D-101 thermogravimetric balance. The gases exited the chamber at a considerable distance above the sample.

At the start of the experiment, the oxygen supply was shut off and the Ar flow rate was set to 1 l min^{-1}. Then a furnace that was already at temperature was raised

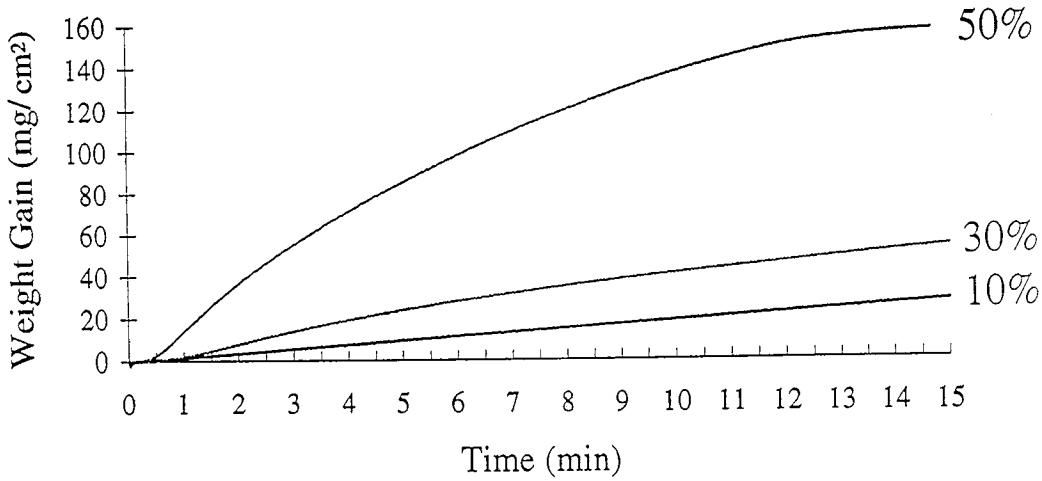

Fig. 1. Weight gain per unit area vs. time plots for WC–6%Co oxidized at 800 °C in Ar–O_2 mixtures of varying oxygen contents of 10%, 30% and 50% at a total flow rate of 1 l min^{-1}.

around the reaction tube. This allowed the sample to rapidly reach the oxidation temperature in an inert atmosphere (it was confirmed that at 800 °C, exposure to Ar for 30 min did not lead to any visible oxidation). After the sample reached the desired temperature, the flow rates of the Ar and O_2 were quickly adjusted to the desired value, and the weight gain of the sample due to oxidation was recorded. Owing to the rapid rate of oxidation, oxidation times for the samples was chosen to be 15 min. After oxidation, the oxygen flow was shut off and the sample was exposed to flowing Ar gas while cooling after the furnace was lowered away from the reaction chamber.

The oxides were examined by scanning electron microscopy (SEM) (JEOL 6100) with an energy dispersive spectroscopy (EDS) attachment, transmission electron microscopy (TEM) (JEOL 200CX), and X-ray diffraction analysis (XRD) (Siemens).

3. Results and discussion

Fig. 1 shows plots of weight gain per unit area vs. time for WC–6%Co samples oxidized at 800 °C in Ar–O_2 mixtures of varying oxygen contents of 10%, 30% and 50%, with a total flow rate in each case of 1 l min^{-1} (from here on, a total flow rate of 1 l min^{-1} will be assumed for all oxidation conditions, unless specifically stated otherwise).

It is clear that increasing the oxygen concentration in the oxidizing atmosphere leads to an increasing rate of oxidation. This indicates that under these conditions, oxygen supply from the atmosphere is rate controlling and not diffusion through the oxide, as is the case for more protective oxides such as Cr_2O_3 and Al_2O_3 [5]. After an initial transient period, the rate of oxidation in 10% and 30% oxygen was found to be linear. The sample for the 50% oxygen case had the fastest oxidation rate and appeared to have a decreasing slope with time. However, this is owing to the fact that the rapid oxidation has caused the surface area of the unreacted WC–Co sample to decrease appreciably from its initial value.

Fig. 2(a) shows the XRD spectrum of the sample exposed to $10O_2/90Ar$. Apart from the substrate WC peaks, the only additional peaks are those of WO_3 and $CoWO_4$. No other oxide phase was detected by this technique. It is interesting to note that the intensity of the {200} WO_3 peak was slightly larger than that of the {001} WO_3 peak. When the oxide was removed and powdered, the peak intensities were reversed as would be expected for randomly oriented WO_3, as shown in Fig. 2(b). This indicates that the WO_3 scale has a very slight {200} texture. Fig. 3 shows SEM images of the oxide surface and cross-section. EDS spectra taken from regions (A) and (B) in Fig. 3(b) identified the phase with the long columnar structure (A) as WO_3 and the dispersed phase (B) as $CoWO_4$. The figure shows that the oxide is highly porous and cracked, which explains the non-protective nature of oxidation. It has been conjectured that the generation of CO and CO_2 during oxidation of WC leads to cracking in WO_3 owing to the force of the escaping gaseous species [6].

It appears that the WO_3 columns in Fig. 3(b) have a width comparable with the WC grain size. Since the Pilling Bedworth ratio (the ratio of the volume of oxide formed to the volume of metal consumed) for W is 3.3 [7], there is a large increase in the volume of the material during oxidation. It is expected that the porous nature of the oxide leads to a much more rapid in-diffusion of oxygen by gas phase diffusion as compared with out-diffusion of W by solid state diffusion. This causes the oxide to be inward growing, i.e. new oxide growth occurs at the oxide/substrate interface. The conversion of WC to the more voluminous WO_3, leads to the growth of WO_3 in columnar fashion, since sideways expansion is restricted by adjacent WO_3 columns. Fig. 4

is a TEM micrograph of a WO_3 column in cross-section, showing a ribbon like sub-structure. Each ribbon is composed of fine WO_3 grains, with considerable amount of porosity between adjacent ribbons.

A portion of the oxide grown on the sample oxidized in $50O_2/50Ar$ is shown in cross-section in Fig. 5. The

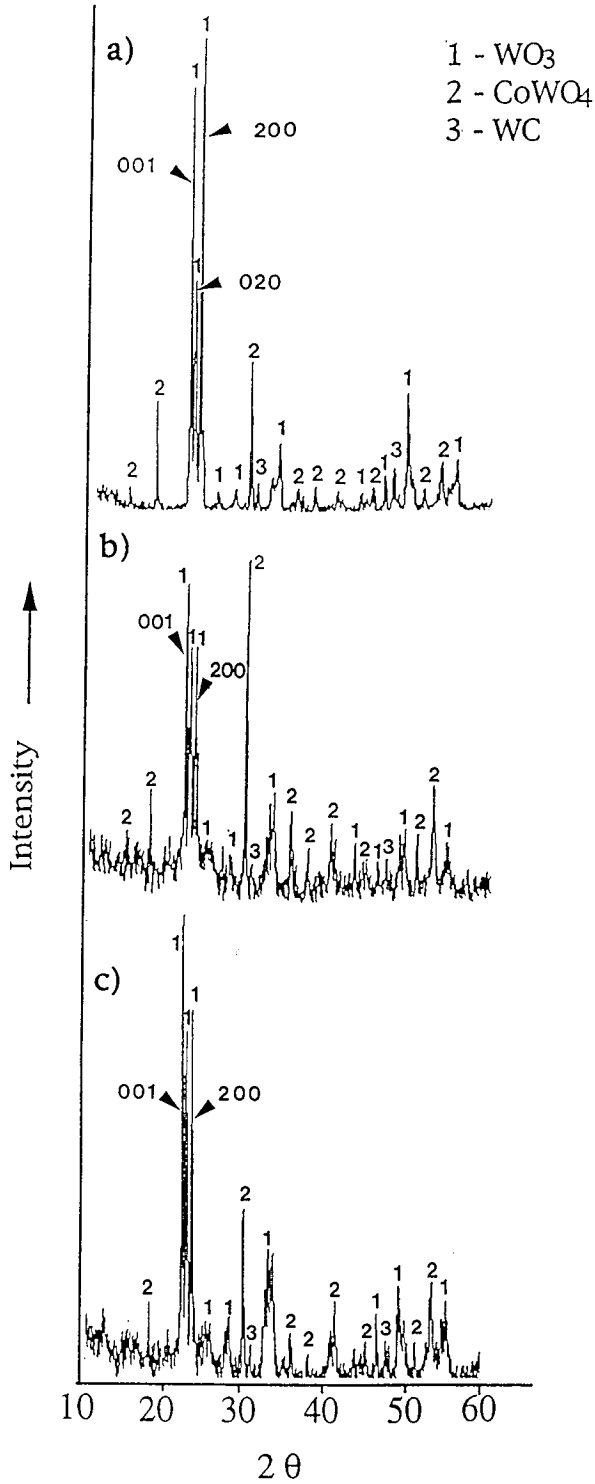

Fig. 2. XRD plots from WC–Co samples oxidized for 15 min at 800 °C for (a) intact oxide formed on 6% Co sample exposed to $10O_2/90Ar$; (b) powdered oxide described in part (a); and (c) intact oxide formed on 12% Co sample exposed to $50O_2/50Ar$.

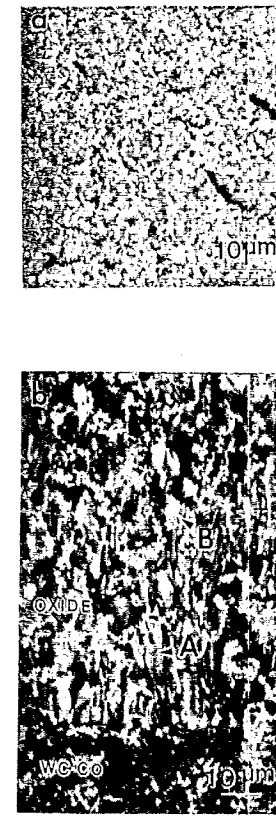

Fig. 3. SEM image of (a) surface and (b) cross-section of oxide formed on 6% Co sample oxidized in $10O_2/90Ar$ at 800 °C for 15 min.

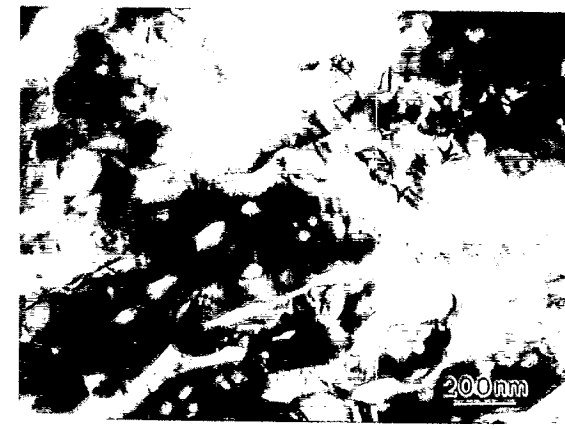

Fig. 4. TEM bright-field image of ribbon-like structure of WO_3 formed on a 6 wt.% Co sample oxidized in $10O_2/90Ar$ at 800 °C for 15 min. Each ribbon consists of fine WO_3 grains with considerable amount of porosity between ribbons.

oxide appears as bands of highly porous and less porous regions, approximately 100 μm in thickness, marked as (A) and (B) respectively in the figure. The EDS spectra from regions (A) and (B) in Fig. 5 show that the W/Co ratio is higher in the more porous region. However, when this oxide was removed and powdered, the relative intensities in the XRD plot were identical to those from powdered oxide formed on the sample exposed to $10O_2/90Ar$. This indicates that the

volume fraction of oxide phases is the same; the only difference is in the morphology of the phases.

Fig. 6 shows the effect of the binder phase on the oxidation behavior of WC–Co. The weight gain plots for 6% and 12% Co samples at 800 °C in a $50O_2/50Ar$ gas mixture, clearly demonstrates that increasing the Co content in WC–Co leads to a reduction of oxidation rate. This can be attributed to a larger volume fraction of $CoWO_4$ phase in the oxide for the 12% Co case. The XRD plot of the powdered oxide scale for this sample is shown in Fig. 2(c) (compare relative intensities of the major $CoWO_4$ with WO_3 peaks in Figs. 2(b) and (c)). Again, these are the only two phases detected in the oxide.

To study the initial (transient) stage of oxidation, a 12 wt.% sample was oxidized at 800 °C for only 1.5 min in a $50O_2/50Ar$ gas mixture. Fig. 7 shows an SEM micrograph of the surface of the sample after the short oxidation exposure. The figure shows the formation of WO_3 islands separated by $CoWO_4$ regions formed over the binder phase. X-ray diffraction analysis shows the presence of {200} texturing of WO_3. This implies that the texturing of WO_3 observed on all samples oxidized at 800 °C is owing to the orientation of the initial oxide formed.

The effect of temperature on the oxidation behavior was also studied. Fig. 8 shows the weight gain per unit area vs. time plots for a 6% Co sample exposed to a $10O_2/90Ar$ gas mixture at temperatures of 600, 700 and 800 °C. The figure shows that the rate of oxidation is almost negligible at 600 °C, with a rapid increase in the oxidation rate at temperature. Fig. 9 shows the surface of the sample after 15 min at 600 and 700 °C respectively. The XRD plots of the oxidized samples are presented in Fig. 10. It is noteworthy that at 600 °C, only WO_3 peaks can be seen. This is probably, because the amount of oxidation is small enough that the volume fraction of the $CoWO_4$ phase is below the detectability limit. Also striking, is the presence of a very strong {001} texture of the WO_3 at 600 °C (the {200} WO_3 peak is almost non-existent). At 700 °C, WO_3 still shows a {001} texturing, although it is not as pronounced as at 600 °C. Thus WO_3 formed during the initial stages of oxidation appears to gradually change from a very strong {001} texturing at 600 °C to a very weak {200} texturing at 800 °C. One concern with the interpretation of the thermogravimetric plots was the possibility of weight loss owing to volatilization of WO_3. It has been reported that WO_3 starts to evaporate under vacuum at 800 °C and the rate becomes significant at 850 °C [8]. In order to investigate the effects of volatilization, an oxidized sample was kept at 800 °C under an inert atmosphere of flowing argon gas for 45 min. No weight loss of the sample was observed indicating that even at the highest temperatures used in this study, WO_3 did not evaporate.

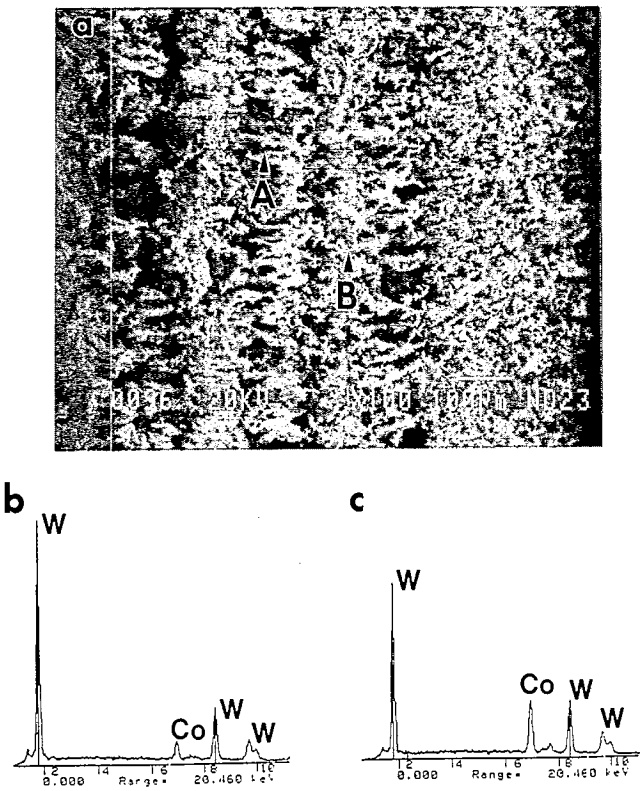

Fig. 5. (a) Cross-section of oxide formed on 6% Co sample oxidized in $50O_2/50Ar$ at 800 °C for 15 min. 100 μm thick regions of porous and dense regions are marked as (A) and (B) respectively. (b) EDS spectra from region (A). (c) EDS spectra from region (B).

The effect of flow rate on oxidation kinetics was also investigated. Fig. 11 shows the weight gain per unit area vs. time for oxidation of 6% Co samples at 800 °C, using a 10% oxygen gas mixture at flow rates of 0.1, 0.4, 1 and 2 l min^{-1}. The figure shows that the rate of oxidation increased with flow rate up to a total flow rate of 1 l min^{-1}. This is not surprising since the non-protective nature of the oxide allows rapid in-diffusion of oxygen to the oxide/sample interface. The rate controlling step is therefore the arrival of oxygen to the interface. Increasing the total flow rate at constant oxygen composition allows a larger arrival rate of oxygen molecules at the interface, leading to enhanced oxidation rates.

Further increase in the total flow rate to 2 l min^{-1} actually led to a decrease in the oxidation rate. There can be two possible explanations for this phenomenon. One reason may be that increasing the flow rate to high values creates a back pressure at the surface, interfering with effective removal of the Co and CO_2 gases generated at the oxide/sample interface owing to oxidation of WC. The increase of partial pressure of these reaction products would slow the oxidation kinetics. The other reason might be an effective reduction of the sample temperature owing to convective cooling by the flowing gas. Since all samples show an increasing rate of oxidation during the initial stages of exposure, it appears that

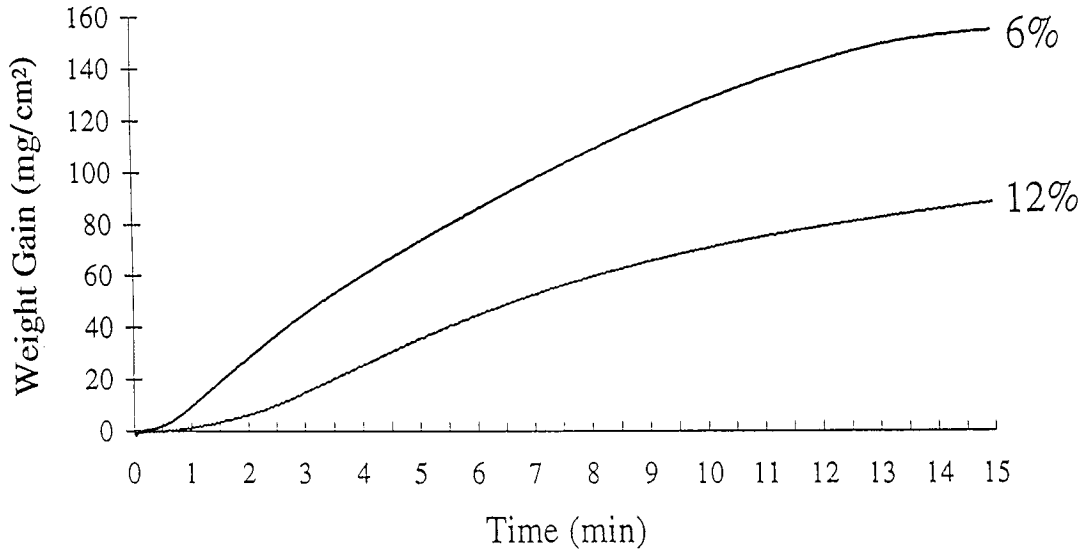

Fig. 6. Weight gain per unit area vs. time plots for 6% and 12% Co samples oxidized at 800 °C in $50O_2/50Ar$ for 15 min.

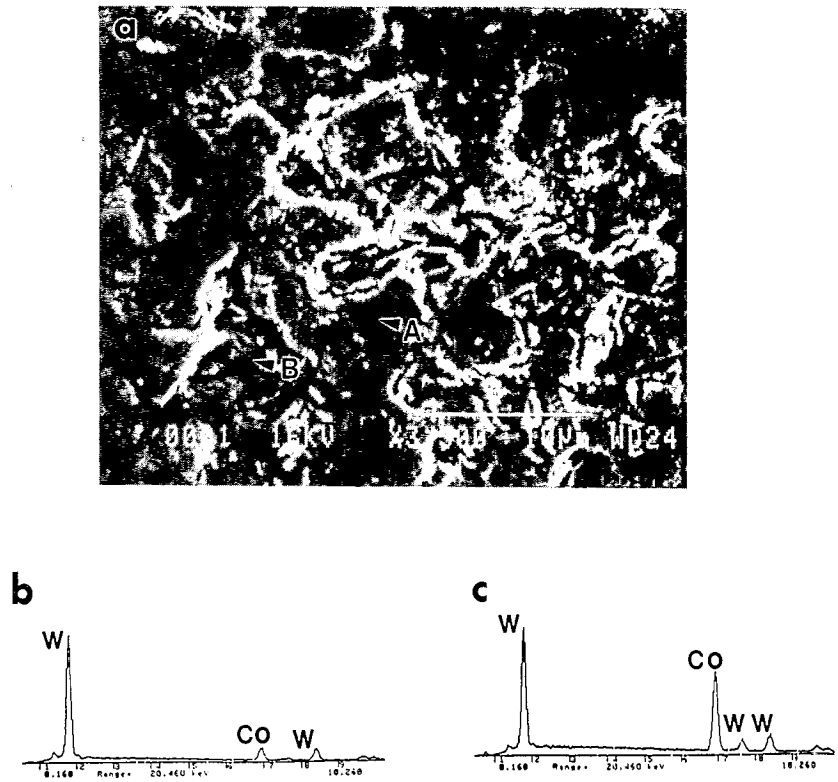

Fig. 7. (a) SEM image of the surface of a 12% Co sample oxidized in $50O_2/50Ar$ at 800 °C for 1.5 min. Oxides formed over a WC grain and over the binder phase is marked as (A) and (B) respectively. (b) EDS spectra from region (A). (c) EDS spectra from region (B).

the latter phenomenon is occurring. If the oxidation rate is indeed limited by the inability of the gaseous products being generated at the interface to escape, the problem of trapping of the reaction gases should be exacerbated by increasing oxide thickness, leading to a decrease in the oxidation rate with time during the initial stages of oxidation. However, the highly exothermic reactions leading to the formation of the oxide products could lead to an increase in the temperature of the sample above the ambient in the furnace. In such a case, the oxidation rate will be auto accelerating, until a steady state temperature is reached. This is what is generally observed. Thus changing flow rates at constant composition has competing effects of oxygen supply to the interface and convective cooling of the sample to the ambient furnace temperature. The former dominates up to a total flow rate of 1 l min^{-1}, leading to an increase in oxidation rate with increasing flow rates. Further increase in the flow rates causes the latter effect to dominate, leading to a reduction in oxidation rate with increasing flow rate.

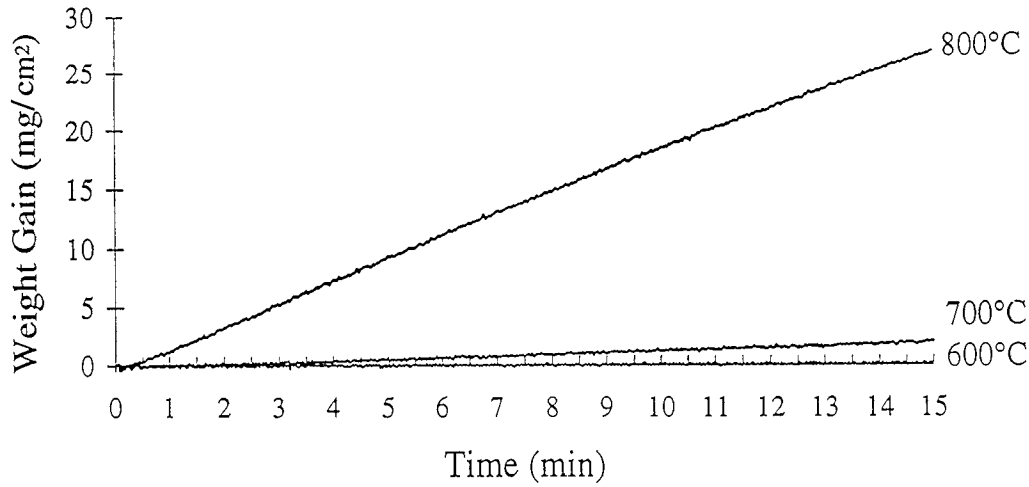

Fig. 8. Weight gain per unit area vs. time plots for 6% Co samples oxidized at 600, 700 and 800 °C in $10O_2/90Ar$ for 15 min.

4. Summary and conclusions

The oxidation behavior of WC–Co samples as a function of oxygen concentration of the atmosphere; Co content in the sample; temperature; and flow rates of the oxidizing gas has been investigated. The oxidation rate of WC–Co was found to be almost negligible at 600 °C, with a rapid increase in the oxidation rate with temperature. The oxidation rate was also observed to increase rapidly with the oxygen content of the atmosphere. An increase in the Co content of the samples led to an improvement in the oxidation behavior. In all cases, the only oxides identified were WO_3 and $CoWO_4$. Although changing the oxidation conditions changed the morphology of the two oxide phases, their relative concentration ratios were determined solely by the Co content of the starting material. The

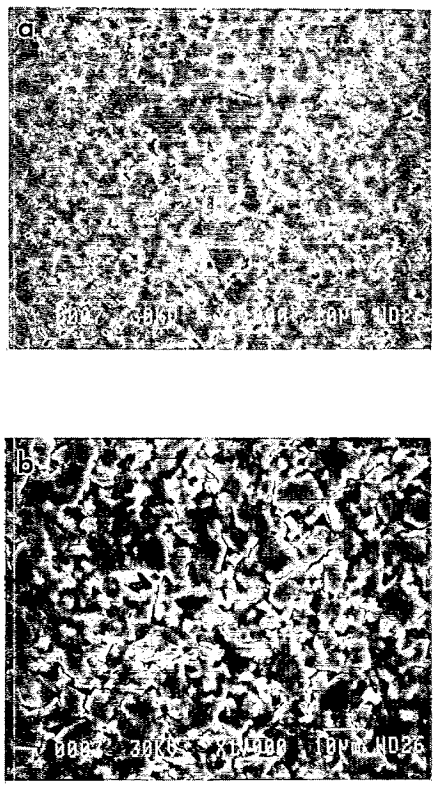

Fig. 9. SEM images of the surface of the 6% Co samples oxidized at (a) 600 °C and (b) 700 °C in 10% oxygen gas mixture at a total flow rate of 1 l min^{-1} for 15 min.

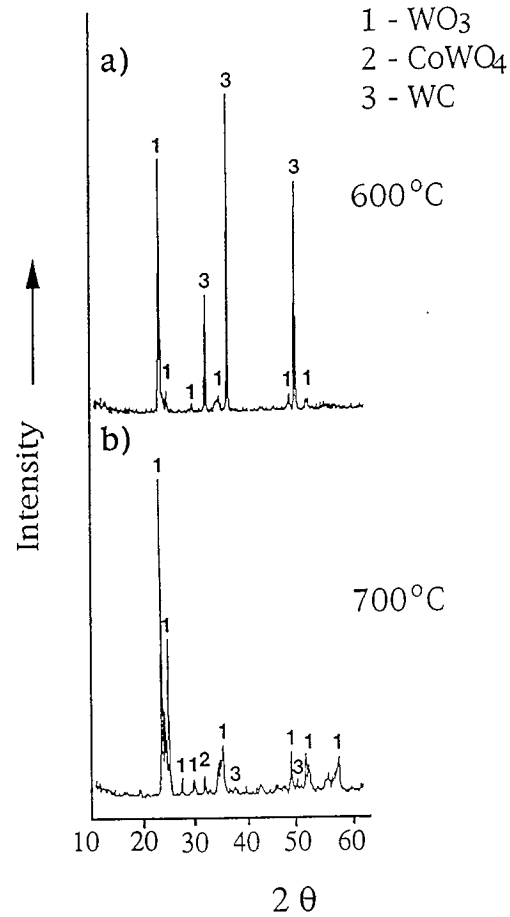

Fig. 10. XRD plots of oxide formed on 6% Co samples oxidized at (a) 600 °C and (b) 700 °C in $10O_2/90Ar$ for 15 min.

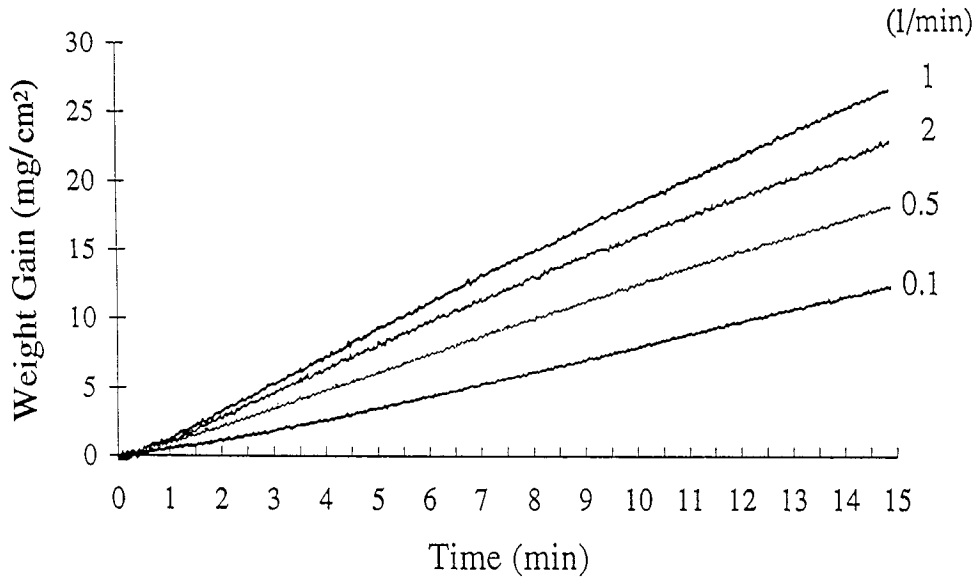

Fig. 11. Weight gain per unit area vs. time plots for 6% Co samples oxidized at 800 °C in $10O_2/90Ar$ at total flow rates of 0.1, 0.5, 1 and 2 l min^{-1} for 15 min.

WO_3 formed during the initial stages of oxidation, changed from a strong {001} texture at 600 °C to a weak {200} texture at 800 °C. As the flow rate of the oxidizing gas was increased, the oxidation rate of WC–Co increased at lower flow rates owing to an increase in the arrival rate of oxygen at the oxide/sample interface. However, at higher flow rates, the oxidation rates decreased with increasing flow rate. It is speculated that this is owing to cooling of the sample from a temperature that is higher than ambient owing to the exothermic nature of the oxidation reaction.

Acknowledgements

The authors gratefully acknowledge the help of their graduate students, C.S. McDowell, D. Doppalapudi and J. Zheng, without whose help the experiments could not have been completed in a relatively short time span.

References

[1] O.Y. Tay, M.G. Stevenson and G. Davis, *Proc. Inst. Mech. Engrs.*, *188* (1974) 627.
[2] V.K. Sarin, in G. Chin (ed.), *Advances in Powder Technology*, ASM, Metals Park, 1982 p. 253.
[3] M.H. Padilla, R.A. Rapp and H.A. Stewart, *Forest Products J.*, *41* (10) (1991) 31.
[4] S.K. Bhaumik, R. Balasubramanium, G.S. Upadhyaya and M.L. Vaidya, *J. Mater. Sci.* (1992) 1457.
[5] G.R. Wallwork, *Rep. Prog. Phys.*, *39* (5) (1976) 29.
[6] W.W. Webb, J.T. Norton and C. Wagner, *J. Electrochem. Soc.*, *103* (2) (1956) 112.
[7] N. Birks and G.H. Meier, *Introduction to High Temperature Oxidation of Metals*, Edward Arnold, London, 1983, p. 119.
[8] E.A. Gulbransen and W.S. Wysong, *Technical Publication No. 2224*, American Institute of Mining and Metallurgical Engineers, New York, NY, 1947.